



**HAL**  
open science

# Magnetic Couplings With Cylindrical and Plane Air Gaps: Influence of the Magnet Polarization Direction

Romain Ravaud, Guy Lemarquand

► **To cite this version:**

Romain Ravaud, Guy Lemarquand. Magnetic Couplings With Cylindrical and Plane Air Gaps: Influence of the Magnet Polarization Direction. Progress In Electromagnetics Research B, 2009, 16, pp.333-349. <10.2528/PIERB09051903>. <hal-00412358>

**HAL Id: hal-00412358**

**<https://hal.science/hal-00412358v1>**

Submitted on 1 Sep 2009

HAL is a multi-disciplinary open access archive for the deposit and dissemination of scientific research documents, whether they are published or not. The documents may come from teaching and research institutions in France or abroad, or from public or private research centers.

L'archive ouverte pluridisciplinaire HAL, est destinée au dépôt et à la diffusion de documents scientifiques de niveau recherche, publiés ou non, émanant des établissements d'enseignement et de recherche français ou étrangers, des laboratoires publics ou privés.



HAL Authorization

## MAGNETIC COUPLINGS WITH CYLINDRICAL AND PLANE AIR GAPS: INFLUENCE OF THE MAGNET POLARIZATION DIRECTION

1 **R. Ravaud, G. Lemarquand**

2 Laboratoire d'Acoustique de l'Universite du Maine, UMR CNRS 6613  
3 Avenue Olivier Messiaen, 72085 Le Mans, France

4 **Abstract**—We present a synthesis of cylindrical magnetic couplings  
5 realized with tile permanent magnets whose polarizations can be  
6 radial, tangential or axial. The expressions of the torque transmitted  
7 between the two rotors of each coupling have been determined by  
8 using the coulombian approach. All the calculations have been  
9 performed without using any simplifying assumptions. Consequently,  
10 the expressions obtained are accurate and enable a fast comparison  
11 between all the structures presented in this paper. Strictly speaking,  
12 there are two great kinds of couplings generally used in engineering or  
13 medical applications. The first ones use a cylindrical air gap though the  
14 second ones use a plane air gap. The best configuration for obtaining  
15 the greatest torque turns out to be different between couplings using  
16 cylindrical or plane air gaps.

### 17 1. INTRODUCTION

18 Up to now, the progress in permanent magnet manufacturing [1]-[3]  
19 have paved the way for the design of very efficient magnetic couplings  
20 [4]-[8] or permanent magnet machines [9]-[15]. Indeed, the assembly of  
21 tile permanent magnets have allowed manufacturers to design devices  
22 that can be easily optimized [17]-[2]. Several approaches [19]-[27] are  
23 used for the study of the torque transmitted between two permanent  
24 magnet rotors [28]-[7]. For performing such optimizations with ana-  
25 lytical approaches, the first step is certainly the determination of the  
26 magnetic field [30][32] produced by the permanent magnet structure.  
27 The analytical calculation of the magnetic field produced by arc-shaped  
28 permanent magnets [33][40] has been largely studied by many authors .  
29 In addition, some authors have proposed series expansions for obtain-  
30 ing a fast evaluation of the magnetic field produced by ring permanent  
31 magnets[41][42] . Such analytical methods are suitable for the design

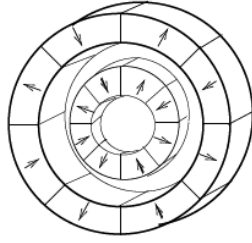


**Figure 1.** Magnetic coupling using a cylindrical air gap and tile permanent magnets radially magnetized

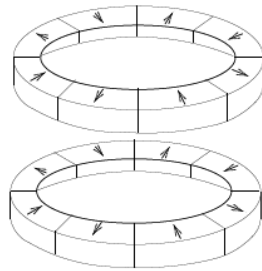


**Figure 2.** Magnetic coupling using a plane gap and tile permanent magnets radially magnetized

32 of non-classical structures using permanent magnets.

33

34 Many papers dealing with the optimization of magnetic couplings  
 35 use the finite element method. However, as mentioned in [43] , it is  
 36 more interesting to use some analytical expressions for calculating the  
 37 magnetic field produced by arc-shaped permanent magnets if such an-  
 38 alytical approaches are possible. We think that it is also the case when  
 39 the calculation of the forces or torques are required.

40

41 The main configurations generally used for realizing magnetic  
 42 couplings are presented below. Indeed, magnetic couplings are  
 43 performed with either cylindrical air gaps, as shown in Fig 1, or with  
 44 plane air gaps, as shown in Fig 2.

45 Some analytical studies have been performed by several authors  
 46 [28]-[44] for studying such magnetic couplings. However, these studies  
 47 omitted the curvature effect of the tile permanent magnets. On the  
 48 other hand, such approaches, based on the linearized model of a mag-

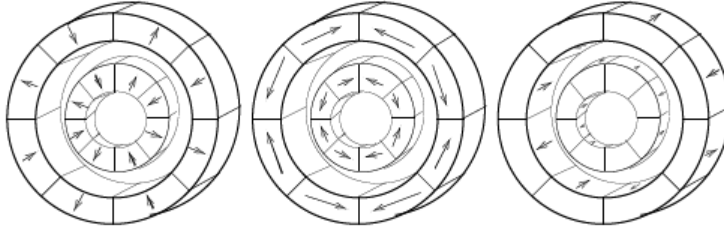


**Figure 3.** Magnetic couplings using cylindrical air gaps; from left to right : coupling using tile permanent magnets radially magnetized, coupling using tile permanent magnets tangentially magnetized, coupling using tile permanent magnets axially magnetized

49 net, are fully analytical and thus interesting to use for optimization  
50 purposes.

51

52 We propose in this paper to use an exact formulation based on the  
53 coulombian model for calculating the torque transmitted bewteen tile  
54 permanent magnets radially, tangentially or axially magnetized. Our  
55 semi-analytical expressions are based on only one numerical integration  
56 whose convergence is fast and robust. All the analytical expressions  
57 have been determined without any simplifying assumptions.

## 58 2. CONFIGURATIONS STUDIED IN THIS PAPER

59 We present in this section the six configurations studied in this paper.  
60 Strictly speaking, our investigation encompasses both the classical  
61 magnetic couplings but also unconventional couplings manufactured  
62 with tile permanent magnets tangentially magnetized. The choice of  
63 the tile permanent magnet polarization depends greatly on the involved  
64 application. Basically, the main criterion for optimizing magnetic  
65 couplings is the value of the torque transmitted between the two rotors.  
66 To do so, several criteria must be taken into account: the media used,  
67 the number and the tile dimensions as well as the intrinsic properties of  
68 the magnets (coercitive field). However, the shape of the torque versus  
69 the angular shift can also be the main optimization criterion. This  
70 is why several configurations of tile permanent magnets with different  
71 polarizations must be compared to each other. We have represented  
72 in Fig 3 three magnetic couplings using only cylindrical air gaps.

73 The three magnetic couplings presented in Fig 3 are composed of  
74 tile permanent magnets radially, tangentially or axially magnetized.

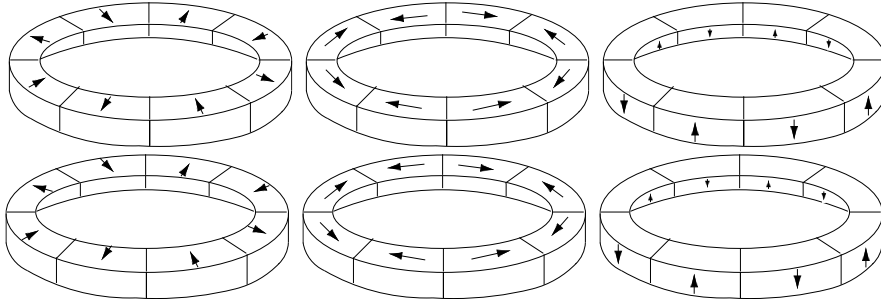


**Figure 4.** Magnetic couplings using plane air gaps; from left to right : coupling using tile permanent magnets radially magnetized, coupling using tile permanent magnets tangentially magnetized, coupling using tile permanent magnets axially magnetized

75 Magnetic couplings using tile permanent magnets radially or axially  
 76 magnetized are rather well known whereas the ones using tile  
 77 permanent magnets tangentially magnetized are less known. The  
 78 magnetic couplings using plane air gaps are presented in Fig 4.

79 The three magnetic couplings presented in Fig 4 are also  
 80 composed of tile permanent magnets radially, tangentially and axially  
 81 magnetized. Such couplings are used in pharmaceutical processes.

### 82 **3. USING THE COULOMBIAN MODEL FOR** 83 **STUDYING THE MAGNETIC COUPLINGS**

84 We present now the three-dimensional equations for the study of the  
 85 structures presented in the previous section.

#### 86 **3.1. Torque transmitted between two tile permanent** 87 **magnets radially magnetized**

88 The torque transmitted between two tile permanent magnets  
 89 radially magnetized is determined by using the analytical expressions  
 90 determined in a previous paper [15]. These analytical expressions are  
 91 based on the coulombian model of a magnet.

#### 92 **3.2. Torque transmitted between two tile permanent** 93 **magnets tangentially magnetized**

94 Let us now consider the torque transmitted between two tile permanent  
 95 magnets tangentially magnetized. The geometry considered and the

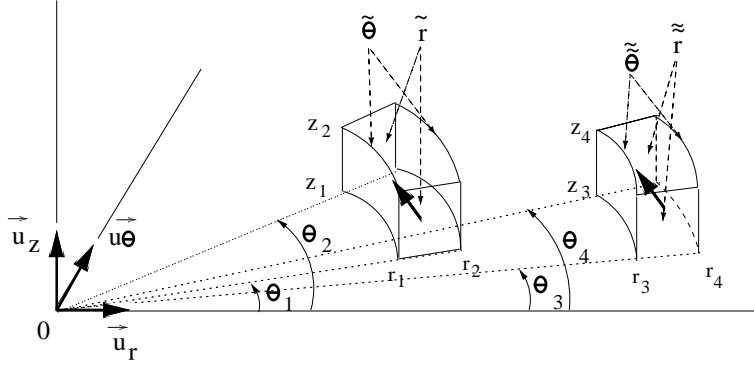


**Figure 5.** Two tile permanent magnets tangentially magnetized

96 related parameters are shown in Fig 5. All the calculations are carried  
 97 out by using the coulombian model. Thus, each tile permanent magnet  
 98 is represented by magnetic pole surface densities that appear only on  
 99 the straight faces of the each tile (Fig 5). For the tile located on the  
 100 left in Fig 5, its inner radius is  $r_1$  and its outer one is  $r_2$ . Its angular  
 101 width is  $\theta_2 - \theta_1$  and its height is  $z_2 - z_1$ . Its magnetic polarization  $\vec{J}_1$   
 102 is directed along  $\vec{u}_\theta$  in cylindrical coordinates. For the tile located on the  
 103 left in Fig 5, its inner radius is  $r_3$  and its outer one is  $r_4$ . Its angular  
 104 width is  $\theta_4 - \theta_3$  and its height is  $z_4 - z_3$ . Its magnetic polarization  $\vec{J}_2$   
 105 is directed along  $\vec{u}_\theta$  in cylindrical coordinates. The torque transmitted  
 106 between the two tile permanent magnets tangentially magnetized is  
 107 determined by integrating the magnetic field produced by the inner  
 108 tile permanent magnet on the magnetic pole surface densities of the  
 109 outer tile permanent magnet. By denoting  $\mathbf{H}(r, \theta, z)$ , the magnetic field  
 110 produced by the inner tile permanent magnet in all points in space,  
 111 the torque transmitted between the two tile permanent magnets can  
 112 be expressed as follows:

$$\begin{aligned}
 T &= J_2 \int_{r_3}^{r_4} \int_{z_1}^{z_2} H_\theta(\tilde{r}, \theta_4, \tilde{z}) \tilde{r} d\tilde{r} d\tilde{z} \\
 &\quad - J_2 \int_{r_3}^{r_4} \int_{z_1}^{z_2} H_\theta(\tilde{r}, \theta_3, \tilde{z}) \tilde{r} d\tilde{r} d\tilde{z}
 \end{aligned} \tag{1}$$

113 where  $H_\theta(r, \theta, z)$  is expressed as follows:

$$H_\theta(r, \theta, z) = -\vec{\nabla} \cdot \left( \int_{r_1}^{r_2} \int_{z_1}^{z_2} G(\vec{r}, \vec{r}') d\phi(\vec{r}') \right) \cdot \vec{u}_\theta \tag{2}$$

114 where  $G(\vec{r}, \vec{r}')$  is the three-dimensional Green's function defined  
115 as follows:

$$G(\vec{r}, \vec{r}') = \frac{1}{4\pi |\vec{r} - \vec{r}'|} \quad (3)$$

116 where  $\vec{r}$  an observation point and  $\vec{r}'$  a point located on the charge  
117 distribution. It is noted that  $G(\vec{r}, \vec{r}')$  has been largely used in [37]. In  
118 addition,  $d\phi(\vec{r}')$  is defined by :

$$d\phi(\vec{r}') = \frac{J_1}{\mu_0} d\tilde{r} d\tilde{z} \quad (4)$$

119 By setting  $x = \cos(\theta_m - \theta_j)$ ,  $y = \sin(\theta_m - \theta_j)$  and  $c = r_i^2 + (z_n - z_k)^2$ ,  
120 the final expression of the torque can be written as follows:

$$T = \sum_{i,j,k,m,n=1}^2 (-1)^{(i+j+k+m+n)} \int_{r_3}^{r_4} \vartheta(\tilde{r}, i, j, k, m, n) d\tilde{r} \quad (5)$$

121 and  $\vartheta(\tilde{r}, i, j, k, m, n)$  is expressed as follows:

$$\begin{aligned} \vartheta(\tilde{r}, i, j, k, m, n) &= \tilde{r}y\sqrt{\tilde{r}^2 + (z_k - z_n)^2 + r_i(r_i - 2\tilde{r}x)} \\ &\quad + \tilde{r}x \log \left[ r_i - \tilde{r}x + \sqrt{\tilde{r}^2 + (z_k - z_n)^2 + r_i^2 - 2r_i\tilde{r}x} \right] \\ &\quad - \frac{(z_k - z_n)(\sqrt{x^2 - 1} - x)}{2\sqrt{x^2 - 1}} \log[A_{i,j,k,m,n}] \\ &\quad - \frac{(z_k - z_n)(\sqrt{x^2 - 1} + x)}{2\sqrt{x^2 - 1}} \log[B_{i,j,k,m,n}] \end{aligned} \quad (6)$$

122

$$\begin{aligned} A_{i,j,k,m,n} &= \frac{-2}{(z_k - z_n)^3} \frac{\left( r_i\tilde{r}(x^2 - 1) - \xi + \tilde{r}^2(x^2 - 1)(\sqrt{x^2 - 1} - x) \right)}{(\sqrt{x^2 - 1} - x)(r_i + \tilde{r}(\sqrt{x^2 - 1} - x))} \\ B_{i,j,k,m,n} &= \frac{-2}{(z_k - z_n)^3} \frac{\left( r_i\tilde{r}(x^2 - 1) + \xi - \tilde{r}^2(x^2 - 1)(\sqrt{x^2 - 1} + x) \right)}{(\sqrt{x^2 - 1} + x)(-r_i + \tilde{r}(\sqrt{x^2 - 1} + x))} \\ \xi &= \sqrt{x^2 - 1}(z_k - z_n) \left( z_k - z_n + \sqrt{r_i^2 + \tilde{r}^2 - 2r_i\tilde{r}x + (z_k - z_n)^2} \right) \end{aligned} \quad (7)$$

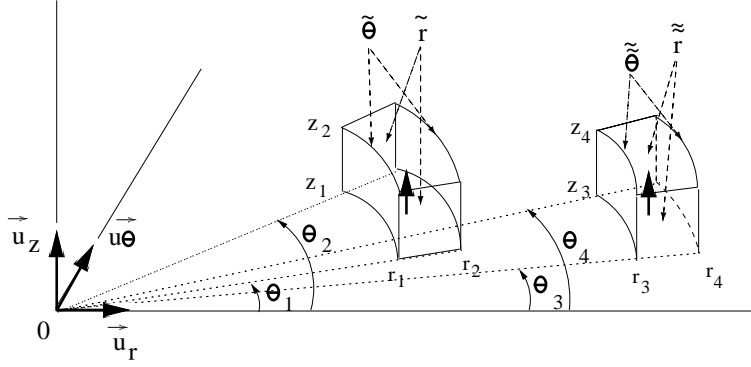


**Figure 6.** Two tile permanent magnets axially magnetized

### 123 3.3. Torque transmitted between two tile permanent 124 magnets axially magnetized

125 The torque transmitted between the two tile permanent magnets  
126 axially magnetized is determined by integrating the magnetic field  
127 produced by the inner tile permanent magnet on the magnetic pole  
128 surface densities of the outer tile permanent magnet. By denoting  
129  $\mathbf{H}(r, \theta, z)$ , the magnetic field produced by the inner tile permanent  
130 magnet in all points in space, the torque transmitted between the two  
131 tile permanent magnets can be expressed as follows:

$$\begin{aligned}
 T &= J_2 \int_{r_3}^{r_4} \int_{\theta_3}^{\theta_3} H_\theta(\tilde{r}, \tilde{\theta}, z_2) \tilde{r} d\tilde{r} d\tilde{\theta} \\
 &\quad - J_2 \int_{r_3}^{r_4} \int_{\theta_3}^{\theta_4} H_\theta(\tilde{r}, \tilde{\theta}, z_1) \tilde{r} d\tilde{r} d\tilde{\theta}
 \end{aligned}
 \tag{8}$$

132 where  $H_\theta(r, \theta, z)$  is expressed as follows:

$$H_\theta(r, \theta, z) = -\vec{\nabla} \cdot \left( \int_{r_1}^{r_2} \int_{\theta_1}^{\theta_2} G(\vec{r}, \vec{r}') d\phi(\vec{r}') \right) \cdot \vec{u}_\theta
 \tag{9}$$

133 where

$$d\phi(\vec{r}') = \frac{J_1}{\mu_0} \tilde{r} d\tilde{r} d\tilde{\theta}
 \tag{10}$$

134 By setting  $\xi = \sqrt{r_i^2 + r_l^2 - 2r_i r_l x + (z_n - z_k)^2}$  and  $\xi_2 = \xi + r_l - r_i x$ ,  
135 the expression of the torque transmitted between two tile permanent

136 magnets axially magnetized can be written as follows:

$$T = \sum_{i,j,k,l,n=1}^2 (-1)^{(i+j+k+l+n)} \int_{\theta_3}^{\theta_4} \vartheta(\tilde{\theta}, i, j, k, l, n) d\tilde{\theta} \quad (11)$$

$$\begin{aligned} \vartheta(\tilde{\theta}, i, j, k, l, n) = & \frac{b^{\frac{3}{2}}x}{3(x^2-1)^{\frac{3}{2}}} \tanh^{-1} \left[ \frac{r_l \sqrt{x^2-1}}{\sqrt{b}} \right] - \frac{r_l^3 x}{9} - \frac{br_l x}{3(x^2-1)} \\ & + \frac{x\xi}{6(x^2-1)} \left( -r_i r_l - 2bx - 3r_i^2 x + r_i r_l x^2 + 3r_i^2 x^3 \right) \\ & + x \log(\xi_2) \left( -\frac{br_i}{2} + \frac{r_i^3 x^2}{2} + \frac{r_i^3}{6} \right) \\ & + \frac{\xi}{6} \left( -r_i r_l x + r_i^2 (2-3x^2) + 2(r_l^2 + (z_n - z_k)^2) \right) \\ & - \frac{\log(\xi_2)}{2} \left( r_i x (r_i^2 (x^2-1) - (z_n - z_k)^2) \right) \\ & + \frac{\left( b^{\frac{3}{2}} r_i x - b^{\frac{3}{2}} r_i x^3 + b^2 x^2 \right) \log(A^I)}{6(x^2-1)^{\frac{3}{2}} \sqrt{bx^2 - 2\sqrt{b}r_i x \sqrt{x^2-1} + r_i^2 (x^2-1)}} \\ & + \frac{\left( -b^{\frac{3}{2}} r_i x + b^{\frac{3}{2}} r_i x^3 + b^2 x^2 \right) \log(A^{II})}{6(x^2-1)^{\frac{3}{2}} \sqrt{bx^2 + 2\sqrt{b}r_i x \sqrt{x^2-1} + r_i^2 (x^2-1)}} \end{aligned} \quad (12)$$

137 By setting  $\alpha^{+,-} = \sqrt{bx^2 \pm 2\sqrt{b}r_i x \sqrt{x^2-1} + r_i^2 (x^2-1)}$ , the parame-  
138 ters  $A^I$  and  $A^{II}$  are defined as follows:

$$\begin{aligned} A^I = & \frac{6(x^2-1)^2 (-r_i^2 + r_i r_l x + r_i^2 x^2 - r_i r_l x^3)}{b^{\frac{3}{2}} (r_l - r_l x^2 + \sqrt{b} \sqrt{x^2-1}) \alpha^- (r_i - r_i x^2 + \sqrt{b} \sqrt{x^2-1})} \\ & + \frac{6(x^2-1)^2 \left( \sqrt{b} (r_l - r_i x) \sqrt{x^2-1} + b(x^2-1) + \xi \sqrt{x^2-1} \alpha^- \right)}{b^{\frac{3}{2}} (r_l - r_l x^2 + \sqrt{b} \sqrt{x^2-1}) \alpha^- (r_i - r_i x^2 + \sqrt{b} \sqrt{x^2-1})} \end{aligned} \quad (13)$$

139

$$A^{II} = \frac{6(x^2-1)^2 (b + r_i^2 - r_i r_l x - bx^2 - r_i^2 x^2 + r_i r_l x^3)}{b^{\frac{3}{2}} \left( \sqrt{b} \sqrt{x^2-1} + r_i (x^2-1) \right) \alpha^+ \left( \sqrt{b} \sqrt{x^2-1} + r_l (x^2-1) \right)}$$

$$+ \frac{6(x^2 - 1)^2 \left( \sqrt{b}(r_l - r_i x) \sqrt{x^2 - 1} - \xi \sqrt{x^2 - 1} \alpha^+ \right)}{b^{\frac{3}{2}} \left( \sqrt{b} x \sqrt{x^2 - 1} + r_i (x^2 - 1) \right) \alpha^+ \left( \sqrt{b} \sqrt{x^2 - 1} + r_l (x^2 - 1) \right)} \quad (14)$$

#### 140 4. COMPARISON OF THREE KINDS OF MAGNETIC 141 COUPLINGS USING A CYLINDRICAL AIR GAP

142 This section presents a comparison between three kinds of magnetic  
143 couplings using cylindrical air gaps. The torque transmitted between  
144 the outer (led rotor) and inner (leading rotor) rotors is determined for  
145 three configurations using 8, 16 and 32 tile permanent magnets. In  
146 other words, the angular widths of each tile permanent magnet are  
147  $\frac{\pi}{4}$  rad,  $\frac{\pi}{8}$  rad,  $\frac{\pi}{16}$  rad,  $\frac{\pi}{32}$  rad and  $\frac{\pi}{64}$  rad. For each tile permanent  
148 magnet, we have  $r_1 = 0.0219$  m,  $r_2 = 0.0249$  m,  $r_3 = 0.025$  m,  
149  $r_4 = 0.028$  m,  $z_1 = 0$  m,  $z_2 = 0.003$  m,  $z_3 = 0$  m,  $z_4 = 0.003$  m.  
150 For the rest of this paper, all the simulations have been carried out  
151 with 2 tile permanent magnets on each rotor.

##### 152 4.1. Simulations

153 The simulations have been carried out with the following dimensions:  
154 each tile permanent magnet has a magnetic polarization that equals  
155 1 T. Their radial width is 3 mm and their height is 3 mm. The air gap  
156 between the two rotors is 0.1 mm. The torque transmitted between the  
157 two rotors is represented versus the angle  $\theta$ , that is, versus the angular  
158 shift between the two rotors.

##### 159 4.2. Discussion

160 Figure 7 shows that tile permanent magnets radially magnetized are  
161 the best solution for having the greatest torque between two rotors with  
162 a cylindrical air gap. However, as tile permanent magnets radially  
163 magnetized are rather difficult to manufacture, it can be interesting  
164 to compare the torque transmitted between two rotors made of tile  
165 permanent magnets tangentially magnetized and two rotors made of  
166 tile permanent magnets axially magnetized. Figure 7 shows that tile  
167 permanent magnets tangentially magnetized are required when the  
168 number of tile permanent magnets used is high (typically superior to  
169 32 for each rotor). When this number is lower, it is more interesting  
170 to use tile permanent magnets axially magnetized.

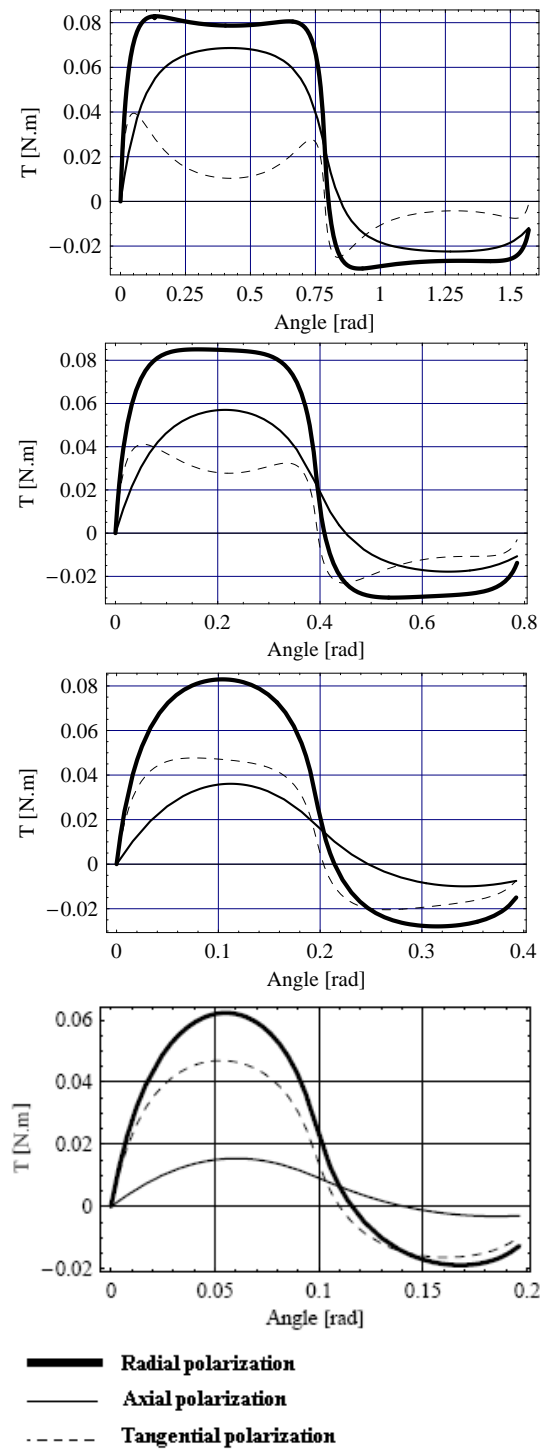


**Figure 7.** Representation of the torque transmitted between two rotors with a cylindrical air gap with tile permanent magnets radially, tangentially and axially magnetized. The angular widths taken are  $\frac{\pi}{4}$  rad,  $\frac{\pi}{8}$  rad,  $\frac{\pi}{16}$  rad and  $\frac{\pi}{32}$  rad respectively from the upper figure to the lower figure

171 **5. COMPARISON OF THREE KINDS OF MAGNETIC**  
 172 **COUPLINGS USING A PLANE AIR GAP**

173 **5.1. Simulations**

174 The simulations have been carried out with the following dimensions:  
 175 each tile permanent magnet has a magnetic polarization that equals  
 176 1 T. Their radial width is 3 mm and their height is 3 mm. The air gap  
 177 between the two rotors is 0.1 mm. For each tile permanent magnet,  
 178 we have  $r_1 = 0.025$  m,  $r_2 = 0.028$  m,  $r_3 = 0.025$  m,  $r_4 = 0.028$  m,  
 179  $z_1 = 0.0031$  m,  $z_2 = 0.0061$  m,  $z_3 = 0$  m,  $z_4 = 0.003$  m.

180 **6. PARAMETRIC STUDY OF THE TORQUE**  
 181 **TRANSMITTED IN CYLINDRICAL AIR GAPS USING**  
 182 **TILE PERMANENT MAGNETS RADIALY, AXIALLY**  
 183 **AND TANGENTIALLY MAGNETIZED**

184 **6.1. Couplings using cylindrical air gaps**

185 We present in this section a parametric study of the torque transmitted  
 186 between the stator and the rotor of a coupling made of two tile perma-  
 187 nent magnets with radial, axial or tangential polarizations located on  
 188 the led and leading parts of this machine. For this purpose, we consider  
 189 first a coupling using a cylindrical air gap with the following dimen-  
 190 sions:  $r_2 - r_1 = 0.003$  m,  $r_4 - r_3 = 0.003$  m,  $z_1 = 0$  m,  $z_2 = 0.003$  m,  
 191  $z_3 = 0$  m,  $z_4 = 0.003$  m,  $J_1 = J_2 = 1$  T,  $\theta_4 - \theta_3 = \theta_2 - \theta_1 = \frac{\pi}{32}$ .

192  
 193 We represent in Figs 9-A, 9-B and 9-C the torque transmitted  
 194 between the leading and led parts of a coupling for four air gaps  
 195 (0.1 mm, 0.3 mm, 0.5 mm, 1 mm). In the three configurations,  
 196 the smallest the air gap is, the greatest the torque is. These figures  
 197 also show that the way the torque decreases versus both the angular  
 198 shift and the air gap is similar for the three polarizations of the tile  
 199 permanent magnets.

200 The other important parameter that can be optimized in a  
 201 magnetic coupling is certainly the thickness of the permanent magnets  
 202 on each parts.

203 We represent in Figs 10-A, 10-B and 10-C the torque transmitted  
 204 between the leading and led parts of a coupling for three magnet  
 205 thicknesses (0.003 m, 0.005 m, 0.011 m). In the three configurations,  
 206 the smallest the magnet thickness is, the greatest the torque is. These  
 207 figures also show that the way the torque decreases versus both the  
 208 angular shift and the air gap is similar for the three polarizations of  
 209 the tile permanent magnets.

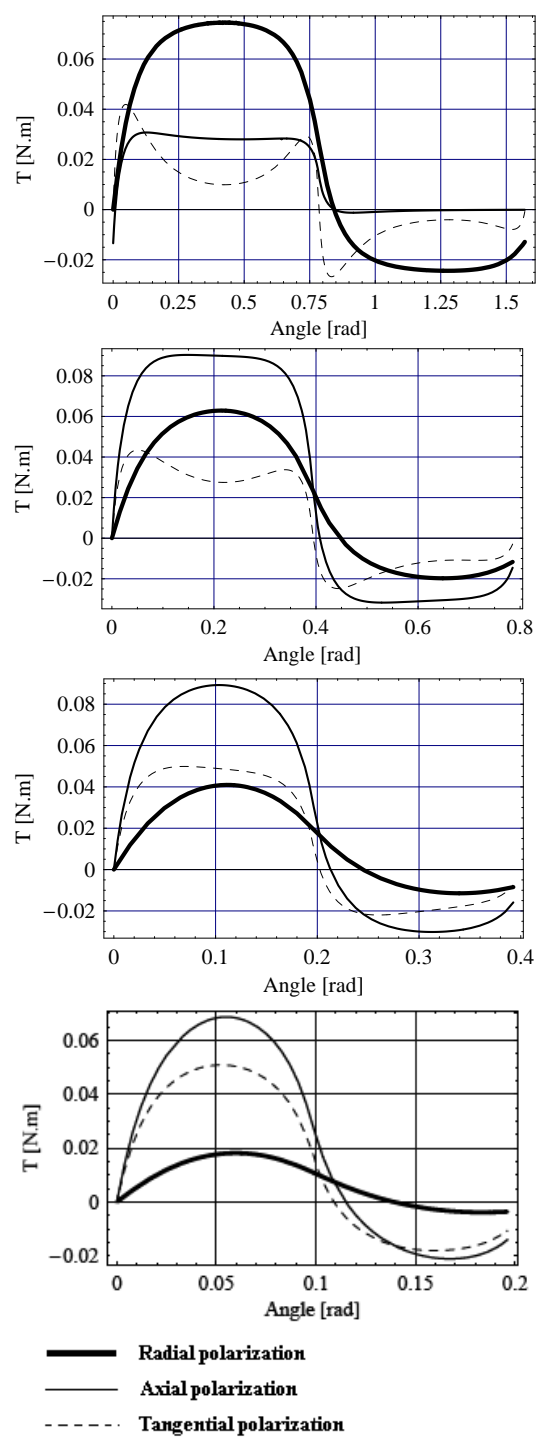


**Figure 8.** Representation of the torque transmitted between two rotors with a plane air gap with tile permanent magnets radially, tangentially and axially magnetized. The angular widths taken are  $\frac{\pi}{4}$  rad,  $\frac{\pi}{8}$  rad,  $\frac{\pi}{16}$  rad and  $\frac{\pi}{32}$  rad respectively from the upper figure to the lower figure

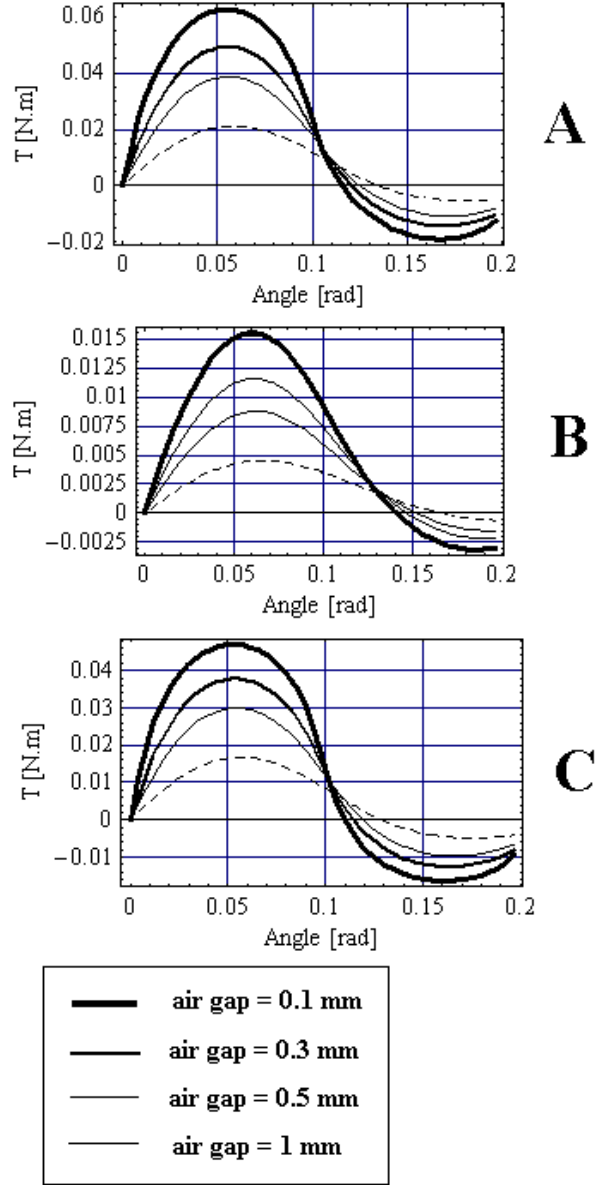


**Figure 9.** Representation of the torque transmitted between two rotors with a cylindrical air gap with tile permanent magnets radially (A), axially (B) and tangentially (C) magnetized with four air gaps (0.1 mm, 0.3 mm, 0.5 mm, 1 mm); we take the following dimensions:  $r_2 - r_1 = 0.003$  m,  $r_4 - r_3 = 0.003$  m,  $z_1 = 0$  m,  $z_2 = 0.003$  m,  $z_3 = 0$  m,  $z_4 = 0.003$  m,  $J_1 = J_2 = 1$  T,  $\theta_4 - \theta_3 = \theta_2 - \theta_1 = \frac{\pi}{32}$

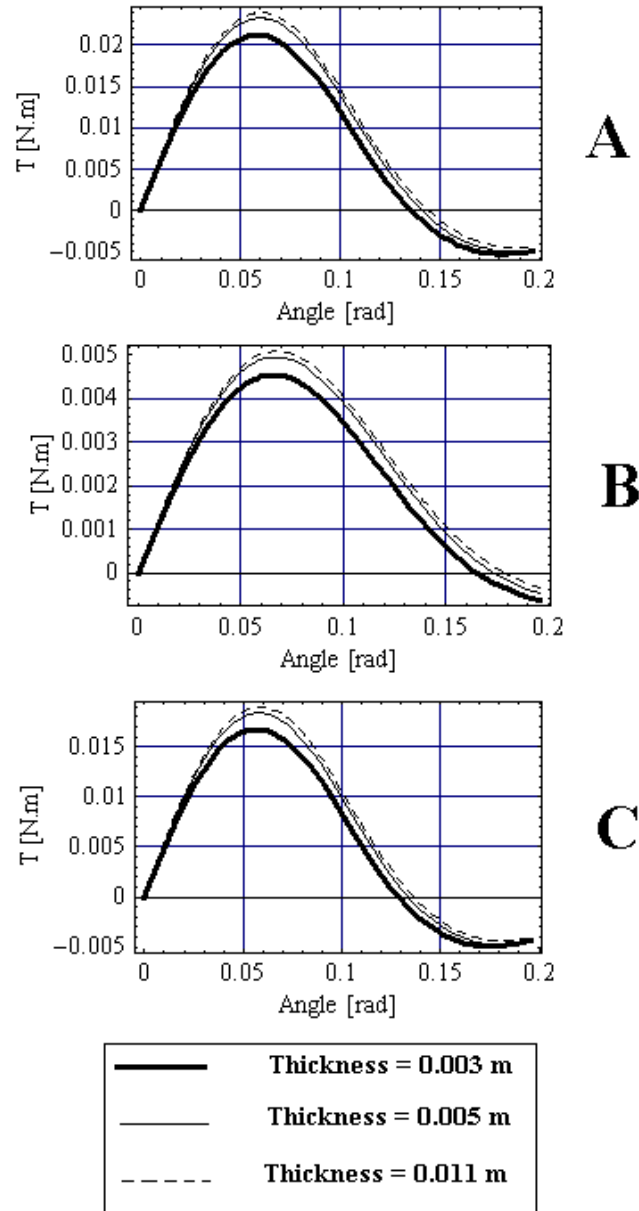


**Figure 10.** Representation of the torque transmitted between two rotors with a cylindrical air gap with tile permanent magnets radially (**A**), axially (**B**) and tangentially (**C**) magnetized with three magnet thickness (0.003 m, 0.005 m, 0.011 m); we take the following dimensions:  $r_2 = 0.024$  m,  $r_3 = 0.025$  m,  $z_1 = 0$  m,  $z_2 = 0.003$  m,  $z_3 = 0$  m,  $z_4 = 0.003$  m,  $J_1 = J_2 = 1$  T,  $\theta_4 - \theta_3 = \theta_2 - \theta_1 = \frac{\pi}{32}$

210 In short, the previous figures show that for a cylindrical coupling,  
211 the air gap must be the smallest and the magnet thickness must be  
212 the greatest and the magnet polarization should be radial.

213

214 We can applied the previous results to the case of plane magnetic  
215 couplings. Indeed, in the case of plane air gaps, the air gap must also  
216 be the smallest, the magnet height must be the greatest and the mag-  
217 net polarization should be axial.

218

## 219 6.2. Discussion

220 Figure 8 shows that tile permanent magnets axially magnetized are  
221 not always the best solution for having the greatest torque between  
222 two rotors with a plane air gap. When the number of tile permanent  
223 magnets used is high, it is more interesting to stack tile permanent  
224 magnets axially magnetized. In the other hand, when the number of  
225 tile permanent magnets used is low, it is more interesting to stack tile  
226 permanent magnets radially magnetized. Furthemore, tile permanent  
227 magnets tangentially magnetized can also be a good compromise what-  
228 ever the number of tile permanent magnets used.

229

230 Figures 9 and 10 present elements of information about how to  
231 optimize cylindrical magnetic couplings with radial, axial or tangen-  
232 tial polarizations. In short, the air gap must always be the smallest  
233 and the magnet thickness should be the greatest. However, the cost  
234 and the weight of the magnet structure must also be taken into account.

235

## 236 7. CONCLUSION

237 This paper has presented a synthesis of magnetic couplings made of  
238 tile permanent magnets radially, tangentially or axially magnetized.  
239 First, we have presented new semi-analytical expressions of the torque  
240 transmitted between two tile permanent magnets tangentially and  
241 axially magnetized. Such a three-dimensional approach allows us  
242 to compare several configurations made of tile permanent magnets  
243 radially, tangentially or axially magnetized. All the calculations have  
244 been carried out without any simplifying assumptions. Therefore,  
245 these expressions are accurate whatever the tile permanent magnet  
246 dimensions. Then, we have proposed to compare magnetic couplings  
247 using cylindrical air gaps and magnetic couplings using plane air gaps.  
248 For the ones using cylindrical air gaps, it is always more interesting

249 to use tile permanent magnets radially magnetized. For the couplings  
 250 using plane air gaps, the most interesting polarization depends greatly  
 251 on the number of tile permanent magnets used. However when the  
 252 angular width of the tile permanent magnet is greater than  $\frac{P_i}{4}$ , the  
 253 axial polarization is the most interesting in the case of plane air gaps.

## 254 REFERENCES

- 255 1. J. P. Yonnet, *Rare-earth Iron Permanent Magnets*, ch. Magneto-  
 256 tomechanical devices. Oxford science publications, 1996.
- 257 2. J. P. Yonnet, S. Hemmerlin, E. Rulliere, and G. Lemarquand,  
 258 “Analytical calculation of permanent magnet couplings,” *IEEE*  
 259 *Trans. Magn.*, vol. 29, no. 6, pp. 2932–2934, 1993.
- 260 3. J. P. Yonnet, “Permanent magnet bearings and couplings,” *IEEE*  
 261 *Trans. Magn.*, vol. 17, no. 1, pp. 1169–1173, 1981.
- 262 4. J. F. Charpentier and G. Lemarquand, “Optimization of  
 263 unconventional p.m. couplings,” *IEEE Trans. Magn.*, vol. 38,  
 264 no. 2, pp. 1093–1096, 2002.
- 265 5. W. Baran and M. Knorr, “Synchronous couplings with sm co5  
 266 magnets,” pp. 140–151, 2nd Int. Workshop on Rare-Earth Cobalt  
 267 Permanent Magnets and Their Applications, Dayton, Ohio, USA,  
 268 1976.
- 269 6. S. M. Huang and C. K. Sung, “Analytical analysis of magnetic  
 270 couplings with parallelepiped magnets,” *Journal of Magnetism*  
 271 *and Magnetic Materials*, vol. 239, pp. 614–616, 2002.
- 272 7. P. Elies and G. Lemarquand, “Analytical study of radial stability  
 273 of permanent magnet synchronous couplings,” *IEEE Trans.*  
 274 *Magn.*, vol. 35, no. 4, pp. 2133–2136, 1999.
- 275 8. R. Ravaud, G. Lemarquand, V. Lemarquand, and C. Depollier,  
 276 “Torque in permanent magnet couplings: comparison of uniform  
 277 and radial magnetization,” *J. Appl. Phys.*, vol. 105, no. 5, 2009.
- 278 9. K. T. Chau, D. Zhang, J. Z. Jiang, and L. Jian, “Transient analysis  
 279 of coaxial magnetic gears using finite element comodeling,”  
 280 *Journal of Applied Physics*, vol. 103, no. 7, pp. 1–3, 2008.
- 281 10. K. T. Chau, D. Zhang, J. Z. Jiang, C. Liu, and Y. Zhang, “Design  
 282 of a magnetic-g geared outer-rotor permanent-magnet brushless  
 283 motor for electric vehicles,” *IEEE Trans. Magn.*, vol. 43, no. 6,  
 284 pp. 2504–2506, 2007.
- 285 11. Z. Zhu and D. Howe, “Analytical prediction of the cogging torque  
 286 in radial-field permanent magnet brushless motors,” *IEEE Trans.*  
 287 *Magn.*, vol. 28, no. 2, pp. 1371–1374, 1992.

- 288 12. M. Aydin, Z. Zhu, T. Lipo, and D. Howe, "Minimization of  
289 cogging torque in axial-flux permanent-magnet machines: design  
290 concepts," *IEEE Trans. Magn.*, vol. 43, no. 9, pp. 3614–3622,  
291 2007.
- 292 13. J. Wang, G. W. Jewell, and D. Howe, "Design optimisation and  
293 comparison of permanent magnet machines topologies," vol. 148,  
294 pp. 456–464, *IEE.Proc.Elect.Power Appl.*, 2001.
- 295 14. L. Yong, Z. Jibin, and L. Yongping, "Optimum design of magnet  
296 shape in permanent-magnet synchronous motors," *IEEE Trans.*  
297 *Magn.*, vol. 39, no. 11, pp. 3523–4205, 2003.
- 298 15. R. Ravaut, G. Lemarquand, V. Lemarquand, and C. Depollier,  
299 "Permanent magnet couplings: field and torque three-dimensional  
300 expressions based on the coulombian model," *IEEE Trans. Magn.*,  
301 vol. 45, no. 4, pp. 1950–1958, 2009.
- 302 16. Y. Li, J. Zou, and Y. Lu, "Optimum design of magnet shape  
303 in permanent-magnet synchronous motors," *IEEE Trans. Magn.*,  
304 vol. 39, no. 11, pp. 3523–4205, 2003.
- 305 17. Y. D. Yao, D. R. Huang, C. C. Hsieh, D. Y. Chiang, S. J.  
306 Wang, and T. F. Ying, "The radial magnetic coupling studies  
307 of perpendicular magnetic gears," *IEEE Trans. Magn.*, vol. 32,  
308 no. 5, pp. 5061–5063, 1996.
- 309 18. M. M. Nagrial, "Design optimization of magnetic couplings using  
310 high energy magnets," *Electric Power Components and Systems*,  
311 vol. 21, no. 1, pp. 115–126, 1993.
- 312 19. E. P. Furlani, "A two-dimensional analysis for the coupling of  
313 magnetic gears," *IEEE Trans. Magn.*, vol. 33, no. 3, pp. 2317–  
314 2321, 1997.
- 315 20. E. P. Furlani, "Field analysis and optimization of ndfeb axial field  
316 permanent magnet motors," *IEEE Trans. Magn.*, vol. 33, no. 5,  
317 pp. 3883–3885, 1997.
- 318 21. E. P. Furlani, S. Reznik, and A. Kroll, "A three-dimensional field  
319 solution for radially polarized cylinders," *IEEE Trans. Magn.*,  
320 vol. 31, no. 1, pp. 844–851, 1995.
- 321 22. E. P. Furlani and T. S. Lewis, "A two-dimensional model for the  
322 torque of radial couplings," *Int J. Appl. Elec. Mech.*, vol. 6, no. 3,  
323 pp. 187–196, 1995.
- 324 23. E. P. Furlani, R. Wang, and H. Kusnadi, "A three-dimensional  
325 model for computing the torque of radial couplings," *IEEE Trans.*  
326 *Magn.*, vol. 31, no. 5, pp. 2522–2526, 1995.
- 327 24. E. P. Furlani, "Formulas for the force and torque of axial  
328 couplings," *IEEE Trans. Magn.*, vol. 29, no. 5, pp. 2295–2301,

- 1993.
- 329
- 330 25. R. Wang, E. P. Furlani, and Z. J. Cendes, "Design and analysis of  
331 a permanent-magnet axial coupling using 3d finite element field  
332 computation," *IEEE Trans. Magn.*, vol. 30, no. 4, pp. 2292–2295,  
333 1994.
- 334 26. E. P. Furlani, "Analysis and optimization of synchronous magnetic  
335 couplings," *J. Appl. Phys.*, vol. 79, no. 8, pp. 4692–4694, 1996.
- 336 27. C. Akyel, S. I. Babic, and M. M. Mahmoudi, "Mutual inductance  
337 calculation for non-coaxial circular air coils with parallel axes,"  
338 *Progress in Electromagnetics Research*, vol. PIER 91, pp. 287–301,  
339 2009.
- 340 28. G. Akoun and J. P. Yonnet, "3d analytical calculation of the forces  
341 exerted between two cuboidal magnets," *IEEE Trans. Magn.*,  
342 vol. 20, no. 5, pp. 1962–1964, 1984.
- 343 29. V. Lemarquand, J. F. Charpentier, and G. Lemarquand,  
344 "Nonsinusoidal torque of permanent-magnet couplings," *IEEE*  
345 *Trans. Magn.*, vol. 35, no. 5, pp. 4200–4205, 1999.
- 346 30. L. Jian and K. T. Chau, "Analytical calculation of magnetic  
347 field distribution in coaxial magnetic gears," *Progress in*  
348 *Electromagnetics Research*, vol. PIER 92, pp. 1–16, 2009.
- 349 31. S. I. Babic, C. Akyel, and M. M. Gavrilovic, "Calculation  
350 improvement of 3d linear magnetostatic field based on fictitious  
351 magnetic surface charge," *IEEE Trans. Magn.*, vol. 36, no. 5,  
352 pp. 3125–3127, 2000.
- 353 32. S. I. Babic and C. Akyel, "Magnetic force calculation between thin  
354 coaxial circular coils in air," *IEEE Trans. Magn.*, vol. 44, no. 4,  
355 pp. 445–452, 2008.
- 356 33. R. Ravaud, G. Lemarquand, V. Lemarquand, and C. Depollier,  
357 "Discussion about the analytical calculation of the magnetic field  
358 created by permanent magnets.," *Progress in Electromagnetics*  
359 *Research B*, vol. 11, pp. 281–297, 2009.
- 360 34. R. Ravaud, G. Lemarquand, V. Lemarquand, and C. Depollier,  
361 "Analytical calculation of the magnetic field created by  
362 permanent-magnet rings," *IEEE Trans. Magn.*, vol. 44, no. 8,  
363 pp. 1982–1989, 2008.
- 364 35. J. P. Selvaggi, S. Salon, O. M. Kwon, and M. V. K. Chari,  
365 "Calculating the external magnetic field from permanent magnets  
366 in permanent-magnet motors - an alternative method," *IEEE*  
367 *Trans. Magn.*, vol. 40, no. 5, pp. 3278–3285, 2004.
- 368 36. S. I. Babic and C. Akyel, "Improvement in the analytical  
369 calculation of the magnetic field produced by permanent magnet

- 370 rings,” *Progress in Electromagnetics Research C*, vol. 5, pp. 71–82,  
371 2008.
- 372 37. R. Ravaud, G. Lemarquand, V. Lemarquand, and C. Depollier,  
373 “The three exact components of the magnetic field created  
374 by a radially magnetized tile permanent magnet.,” *Progress in*  
375 *Electromagnetics Research*, *PIER 88*, pp. 307–319, 2008.
- 376 38. R. Ravaud and G. Lemarquand, “Analytical expression of the  
377 magnetic field created by tile permanent magnets tangentially  
378 magnetized and radial currents in massive disks,” *Progress in*  
379 *Electromagnetics Research B*, vol. 13, pp. 309–328, 2009.
- 380 39. R. Ravaud and G. Lemarquand, “Discussion about the magnetic  
381 field produced by cylindrical halbach structures,” *Progress in*  
382 *Electromagnetics Research B*, vol. 13, pp. 275–308, 2009.
- 383 40. R. Ravaud, G. Lemarquand, V. Lemarquand, and C. Depollier,  
384 “Magnetic field produced by a tile permanent magnet whose  
385 polarization is both uniform and tangential,” *Progress in*  
386 *Electromagnetics Research B*, vol. 13, pp. 1–20, 2009.
- 387 41. O. M. Kwon, C. Surussavadee, M. V. K. Chari, S. Salon, and K. S.  
388 Vasubramaniam, “Analysis of the far field of permanent magnet  
389 motors and effects of geometric asymmetries and unbalance in  
390 magnet design,” *IEEE Trans. Magn.*, vol. 40, no. 3, pp. 435–442,  
391 2004.
- 392 42. E. Perigo, R. Faria, and C. Motta, “General expressions for the  
393 magnetic flux density produced by axially magnetized toroidal  
394 permanent magnets,” *IEEE Trans. Magn.*, vol. 43, no. 10,  
395 pp. 3826–3832, 2007.
- 396 43. B. Azzerboni, G. A. Saraceno, and E. Cardelli, “Three-  
397 dimensional calculation of the magnetic field created by current-  
398 carrying massive disks,” *IEEE Trans. Magn.*, vol. 34, no. 5,  
399 pp. 2601–2604, 1998.
- 400 44. F. Bancel and G. Lemarquand, “Three-dimensional analytical  
401 optimization of permanent magnets alternated structure,” *IEEE*  
402 *Trans. Magn.*, vol. 34, no. 1, pp. 242–247, 1998.